

Nonlocal screening effects in 2p x-ray photoemission spectroscopy of NiO (100)

D. Alders

Department of Applied and Solid State Physics, Materials Science Centre, University of Groningen, Nijenborgh 4, 9747 AG Groningen, The Netherlands

F. C. Voogt and T. Hibma

Department of Chemical Physics, Materials Science Centre, University of Groningen, Nijenborgh 4, 9747 AG Groningen, The Netherlands

G. A. Sawatzky

Department of Applied and Solid State Physics, Materials Science Centre, University of Groningen, Nijenborgh 4, 9747 AG Groningen, The Netherlands

(Received 1 March 1996)

We report on the layer thickness dependence of Ni 2p core-level line shapes of epitaxially grown, in a layer-by-layer fashion, NiO on a single-crystal MgO (100) substrate. The results demonstrate the sensitivity of the core-level line shape to the nearest as well as next-nearest-neighbor coordination number. The results are consistent with a recent theoretical study of nonlocal screening effects. [S0163-1829(96)08032-0]

I. INTRODUCTION

The interest in the electronic structure of bulk NiO has a long-standing history and will most likely be the subject for further discussions in the future. It started with de Boer and Verwey¹ in 1937, when they pointed out that the observed band gap was in disagreement with predictions of elementary band structure theory.^{2,3} The insulating nature was originally explained by the Mott-Hubbard picture, where the correlation gap is induced by the large 3d-3d Coulomb interactions.^{4,5} After this it took almost 50 years to realize that the band gap is of a charge-transfer type, involving explicitly the surrounding ligands.⁶⁻⁸

Even today there are still a lot of open questions left, like for instance the experimentally observed catalytic properties of this material.⁹⁻¹¹ Some authors have examined the absorption of hydrogen or CO on the surface of NiO using the cluster method model of the (100) surface. It was concluded that the perfect surface is almost inert, but that defects in first and second layers provide a variety of active sites for chemisorption.¹²

One technique being used to study the surface of NiO is core-level x-ray photoemission spectroscopy (XPS), at the Ni 2p edge. Although the satellite structure, at about 1.5-eV higher binding energy with respect to the main peak, has been known for decades, the origin thereof is still open for discussion; see Ref. 13 and references therein. In connection with the identification of defect structures, this satellite in the Ni 2p XPS spectrum has conventionally been assigned to Ni³⁺ species existing on the surface. However, the intrinsic appearance even for freshly cleaved single crystals¹³ and the use of x-ray-absorption spectroscopy (XAS) (Ref. 14) made this interpretation doubtful. In addition, the increase of this peak after successive sputter cycles is surprising; since defects are characterized by anion vacancies therefore a reduction of the Ni valency is expected.¹⁵ Some authors have tried to assign this peak to $\underline{c}d^{10}\underline{L}^2$ (Ref. 16) or $\underline{c}3d^9$ multiplet

structures.¹⁷ However, if one assumes either of these explanations to be the correct one, it is hard to explain the absence of this peak in highly diluted Ni samples in MgO,¹⁸ because in these samples the Ni ions are also octahedrally surrounded by oxygen.

Recently, a theoretical interpretation was proposed by Van Veenendaal and Sawatzky,¹⁹ explaining both the intrinsic appearance and the sensitivity to defects. They showed that 2p core-level line shapes of transition-metal compounds, in general, are strongly influenced not only by nearest-neighbor but also next-nearest-neighbor configurations, and therefore strongly depend on the details of the structure. In this paper we present experimental support for this latter explanation.

II. EXPERIMENT

The NiO samples were epitaxially grown, in a layer-by-layer fashion on a single crystal MgO (100) substrate. The method used has been described previously.²⁰ Both NiO and MgO exhibit the face-centered-cubic ‘‘rocksalt’’ (NaCl) crystalline structure, with lattice constants of 4.176 and 4.212 Å, respectively, which result in a 0.85% lattice mismatch. The substrate was cleaved *ex situ*, yielding a platelet of $\approx 10 \times 10$ mm², and was cleaned by heating for 12 h at 600 °C to remove hydrocarbons from the surface. Ni was evaporated from a Knudsen cell at 1300 °C, and growth of NiO was accomplished using an oxidizing agent of NO₂. Layer thickness and sample characterization was done by reflection high-energy electron diffraction.

The XPS measurements reported here were made in two different UHV systems. *In situ* measurements, in a separate analysis chamber, were made directly after film growth, with a nonmonochromatized Al K α x-ray source and a VG Clam2 analyzer. The base pressure in this analysis chamber system was 1×10^{-10} Torr. All spectra were recorded with a spot diameter of ≈ 8 mm and an energy resolution of 1.1 eV,

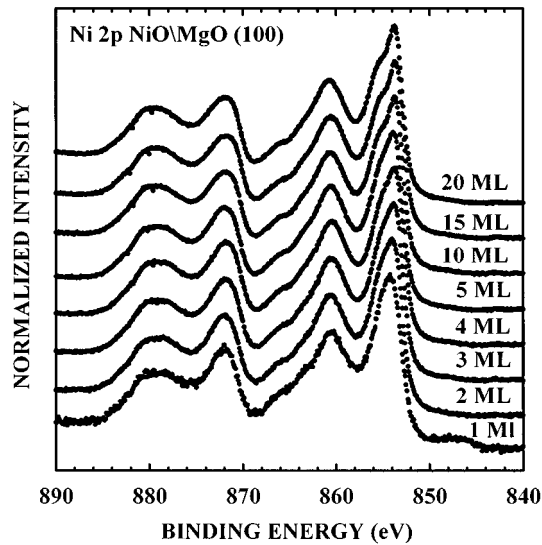


FIG. 1. Experimental Ni $2p$ XPS spectra of epitaxially grown, in a layer-by-layer fashion, NiO on single crystal MgO (100), at room temperature. From top to bottom the spectra of 20, 15, 10, 5, 4, 3, 2, and 1 ML are shown. See Fig. 3 for corresponding O $1s$ XPS spectra. Note the change in the higher binding satellite structure at ≈ 1.5 eV above the main line, in both $2p_{1/2}$ and $2p_{3/2}$ edges.

determined by the core levels of sputtered Ag. After data collection the spectra were filtered to remove the satellite structure of the nonmonochromatic Al $K\alpha$ radiation. *Ex situ* measurements were performed with a small spot XPS (with a spot size of $300 \mu\text{m}$ and an energy resolution of 0.7 eV) using a monochromatized Al $K\alpha$ source. Since all samples exhibited charging effects, the spectra presented here were corrected for this. To do this we assumed a constant O $1s$ binding energy of 529.4 eV as a reference.

The experimental XAS data reported here have been obtained using the AT&T Bell Laboratories Dragon Beam line at the National Synchrotron Light Source.²¹ The spectrum shown is recorded with the total electron yield method.

III. RESULTS

The layer thickness dependence of Ni $2p$ XPS spectra of epitaxially grown NiO on a single-crystal MgO (100) substrate is shown in Fig. 1. The spectrum can be roughly divided into two edges split by spin-orbit coupling, referred to as the $2p_{1/2}$ (≈ 870 – 885 eV) and $2p_{3/2}$ (≈ 850 – 869 eV) edges, respectively. The current understanding of the Ni $2p$ XPS spectrum of NiO $3d^8$ is shown schematically on the left-hand side of Fig. 2. The creation of a hole in the $2p$ core level of the transition-metal site is accompanied by a strong Coulomb repulsion with the holes in the localized $3d$ orbitals. The lowest energy will then be of $\underline{c}3d^9\underline{L}$, whereas the ground state is of predominantly $3d^8$ character, where \underline{c} and \underline{L} refer to a hole in the $2p$ core level and the ligand band, respectively. The satellite structure at higher binding energies (≈ 858 – 870 eV) can be assigned to the unscreened $\underline{c}d^8$ and screened $\underline{c}d^{10}\underline{L}^2$ final states. The most important feature for the discussion here is the satellite peak at approximately 1.5 eV higher binding energy of the main line in both edges. This peak *cannot* be explained within the model de-

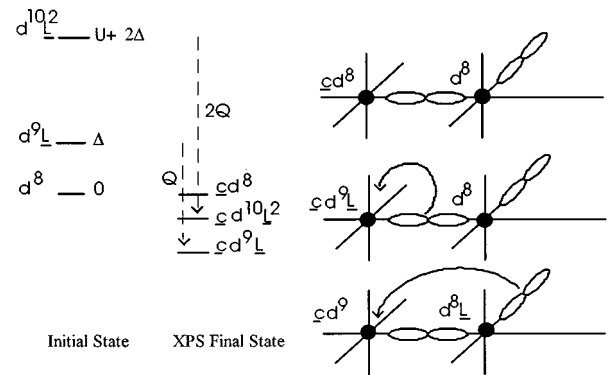


FIG. 2. On the left-hand side we show the energy-level scheme in the XPS initial and final states. On the right-hand side we show (top) two metal ion sites with a core hole on one site (middle) screening of an electron from the surrounding oxygen ligands, and (bottom) nonlocal screening from an electron from a neighboring unit.

scribed. Therefore a more extended explanation has been proposed by Van Veenendaal and Sawatzky.¹⁹ They considered clusters consisting of more than one transition-metal ion. This allows the metal sites and ligands to interact. A consequence of this is that a core hole can also be screened by an electron coming from a neighboring NiO₆ unit, and does not necessarily have to come from the ligands at the core-hole site. This type of screening mechanism which requires at least two sites is referred to as nonlocal screening. In the data presented here one can clearly see a layer thickness dependence of the satellite at ≈ 1.5 eV, while all other features in the spectrum are well reproduced and, in first order, do not depend on the sample thickness.

In Fig. 3 we also show the accompanying layer thickness dependence of the O $1s$ XPS spectra. All spectra consist of

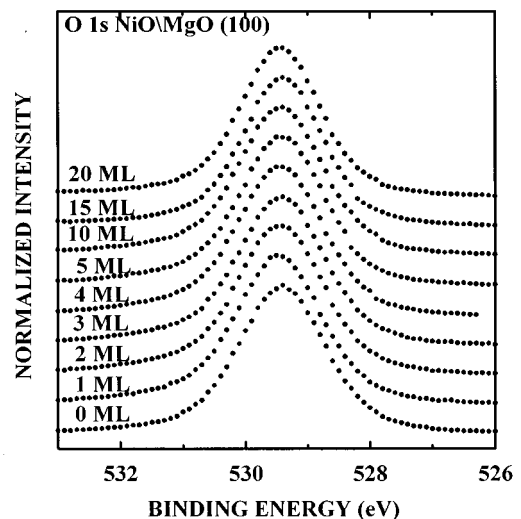


FIG. 3. Experimental O $1s$ XPS spectra of epitaxially grown, in a layer-by-layer fashion, NiO on single-crystal MgO(100), at room temperature. From top to bottom the spectra of 20, 15, 10, 5, 4, 3, 2, and 1 ML are shown. See Fig. 1 for corresponding Ni $2p$ XPS spectra. Note the absence of any shoulder or satellite structure.

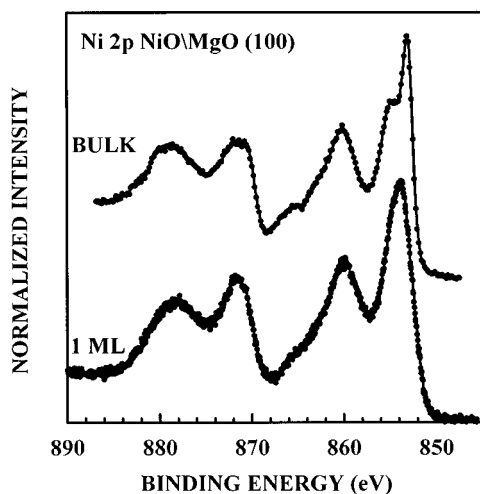


FIG. 4. Experimental Ni 2*p* XPS spectra of epitaxially grown, in a layer-by-layer fashion, NiO on single-crystal MgO (100) at room temperature using a higher-resolution spectrometer. From top to bottom the spectra of bulk and 1 ML are shown. Due to the better resolution used here the change in the higher binding satellite structure at ≈ 1.5 eV above the main line is more pronounced. See Fig. 1 for a comparison.

only one peak, which does not have any satellite structure. This demonstrates that the studied surfaces are clean, because oxygen-related compounds like H₂O or OH groups would give rise to higher binding-energy satellites. There is no indication of layer thickness dependence; apparently this core level does not depend on neighboring coordination. This is because the O 2⁻ (2*p*⁶) band is almost full. The conclusion is that the O 1*s* peak of clean well-ordered NiO surfaces is a single peak, and does not depend on layer thickness.

Unfortunately the visibility of the effect shown in Fig. 1 is limited by the resolution of the XPS analyzer in the molecular-beam epitaxy (MBE) system. To stress that the change observed is not a small effect, in Fig. 4 we show Ni 2*p* XPS data taken with a better resolution. These data have been obtained after transport, through air, of samples grown in the MBE system to a system with a better resolution. The layer thickness dependence in both figures is essentially the same; only the effect is more pronounced in the latter, because of the better resolution. The O 1*s* edge for these samples, not shown here, does show a small peak at higher binding energy due to oxygen-related contaminants at the surface.

A typical Ni 2*p* x-ray absorption spectrum of a thin epitaxially grown film of NiO on MgO (100) is shown in Fig. 5; we refer to Ref. 22 for a more elaborate analysis of this film. The point we want to make here is that XAS is an element-specific technique, which for 3*d* transition-metal compounds is extremely sensitive to the valency of the specimen under study.²³ Therefore one can unambiguously determine the formal valency to be Ni²⁺. This experimental observation is in contradiction with the assumption that the doubly peaked main line observed with XPS is due to Ni³⁺ ions.²⁴

IV. DISCUSSION

The theoretical interpretation of the Ni 2*p* XPS edge of NiO (100) by Van Veenendaal and Sawatzky¹⁹ is supported

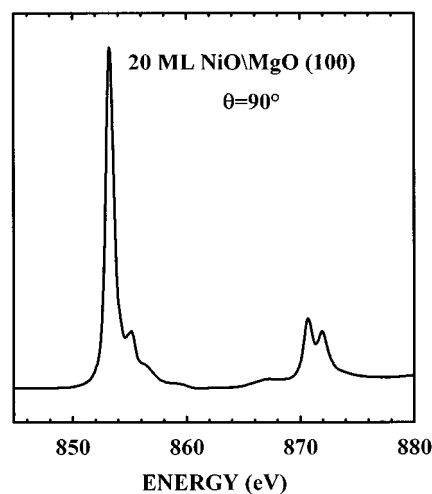


FIG. 5. Experimental Ni 2*p* XAS spectrum of epitaxially grown NiO on single-crystal MgO (100) at room temperature.

by the experiments shown in this paper. Their interpretation is based on (multiple site) cluster calculations, which show that the satellite structure, at 1.5-eV higher binding energy above the main line in Ni 2*p* XPS, is intrinsic for this compound. Moreover, this interpretation approximately gives the correct energy position and intensity. The satellite peak is the result of a screening process by an electron that does not come from the oxygen orbitals around the Ni with the core hole, but from a neighboring NiO₆ unit. The screening mechanism is schematically shown on the right-hand side of Fig. 2. After the creation of a core hole $d^n \rightarrow \underline{c}d^n$, the energy of the system can be lowered by screening electrons from neighboring sites. This yields $\underline{c}d^n \rightarrow \underline{c}d^{n+1}\underline{L}$ and higher-order states, where \underline{L} in most calculations refers to a hole in the ligand band limited to a single transition-metal ion site, as an impurity or surrounded only by ligand atoms in a cluster. Nonlocal screening involves at least two sites, and is the process where an electron is transferred from a neighboring NiO₆ unit $\underline{c}d^n; d^n \rightarrow \underline{c}d^{n+1}; d^n \underline{L}$. In the case of NiO this yields a local configuration of mainly 2*p*⁵3*d*⁹ character at the core-hole site, and an extra hole 3*d*⁸ \underline{L} in a neighboring unit. This also nicely explains the absence of this peak in diluted samples,¹⁸ since then there are no neighboring Ni sites present for this type of screening mechanism. Since NiO is a charge-transfer insulator, the extra valence holes reside primarily on the oxygen orbitals around the Ni site, as is clearly shown in a related compound by the O 1*s* XAS data²⁵ of Li_{*x*}Ni_{1-*x*}O. This hole couples antiferromagnetically to the two other holes, forming a local ²*E* symmetry state around the center.

The change in the layer thickness dependence of the satellite intensity found experimentally can be related to the change in local structure, since the intensity is a result of the interplay between local and intersite screening. As predicted by the calculations, nonlocal screening is more important for surface than for bulk atoms. This subtle mechanism also explains why there is no consensus about the experimental results reported in the literature, since the height of the satellite is an intrinsic function of the local environment and is therefore extremely sensitive to sample preparation, defects, and surface crystallinity.

The size of the calculation required to describe this non-local screening effect correctly prohibits a detailed comparison with experiment, although the effect itself and the influence on the Ni $2p$ spectra can be clearly demonstrated. Changes in the model parameters at the surface, as for instance the charge transfer energy Δ , which is a function of the Madelung potential, makes a detailed comparison difficult. Note that if this comparison were possible, one could obtain a correlation length between the site where the core hole was created and the so-called nonlocal screening unit. This $d^n\bar{L}$ state is only weakly bound to the core-hole site, and therefore is in principle free to move through the lattice.

In this paper we give experimental support for the fact that the satellite peak in the Ni $2p$ XPS spectrum is intrinsic for NiO. The theory, also taking into account nonlocal screening effects, is able to explain the observed satellite structure, and therefore we do not need the assumption of the existence of defect structure (Ni^{3+}) at the surface. Defects in NiO are related to the loss of oxygen, which effects the local coordination number. This lowering of the symmetry leads to a more reasonable assumption about the existence of electron-doped units in defective NiO, since in this case Ni is not able to donate two electrons to the surrounding oxygens. In this case $\text{Ni}^{1+} 3d^9$ units are formed, which could be the active centers in a catalytic reaction.

V. CONCLUSIONS

In conclusion we have shown the layer thickness dependence of the satellite structure in Ni $2p$ photoemission spectra of epitaxially grown NiO on a single crystal MgO (100) substrate. The relative intensity change of the satellite with respect to the main line can be explained by a theory presented in Ref. 19, and is caused by a competition between screening electrons coming from the surrounding ligands and electrons coming from ligands around a neighboring transition-metal ion. Experimental XAS data do not support the existence of Ni^{3+} at the surface. The existence of electron-doped units in defective NiO (100) structures is more likely, and might give some new additional insight in the catalytic mechanism.

ACKNOWLEDGMENTS

This work was financially supported by the Nederlandse Stichting voor Fundamenteel Onderzoek der Materie (FOM) and the Stichting Scheikundig Onderzoek in Nederland (SON), which are supported by the Nederlandse Organisatie voor wetenschappelijk Onderzoek (NWO).

-
- ¹H.J. de Boer and E.J.W. Verwey, Proc. Phys. Soc. A **49**, 59 (1937).
²F. Bloch, Z. Phys. **57**, 454 (1929).
³A.H. Wilson, Proc. R. Soc. London Ser. A **133**, 458 (1931).
⁴N.F. Mott, Proc. Phys. Soc. A **62**, 416 (1949).
⁵J. Hubbard, Proc. R. Soc. London Ser. A **277**, 237 (1964).
⁶A. Fujimori and F. Minami, Phys. Rev. B **30** 957 (1984).
⁷G.A. Sawatzky and J.W. Allen, Phys. Rev. Lett. **53**, 2339 (1984).
⁸S. Hüfner, J. Ostwalder, T. Riesterer, and F. Hulliger, Solid State Commun. **52**, 793 (1984).
⁹P.C. Gravelle and S.J. Teichner, Adv. Catal. **20**, 167 (1969).
¹⁰G. Pacchioni, G. Cogliandro, and P.S. Bagus, Surf. Sci. **255**, 344 (1991).
¹¹J. Freitag and V. Staemmler, J. Electron Spectrosc. Relat. Phenom. **69**, 99 (1994).
¹²J.M. Blaisdell and A.B. Kunz, Phys. Rev. B **29**, 988 (1984).
¹³St. Uhlenbrock, Chr. Scharfschwerdt, M. Neumann, G. Illing, and H.-J. Freund, J. Phys. Condens. Matter **4**, 7973 (1992).
¹⁴L. Soriano, M. Abbate, J. Vogel, J.C. Fuggle, A. Fernández, A. R. González-Elipe, M. Sacchi, and J.M. Sanz, Chem. Phys. Lett. **208**, 460 (1993).
¹⁵J.M. McKay and V.E. Henrich, Phys. Rev. B **32**, 6764 (1975).
¹⁶M. Oku, H. Tokuda, and K. Hirokawa, J. Electron. Spectrosc. **53**, 201 (1991).
¹⁷K.S. Kim and R.E. Davis, J. Electron. Spectrosc. **1**, 251 (1972).
¹⁸M. Oku and K. Hirokawa, J. Electron. Spectrosc. **10**, 103 (1977).
¹⁹M.A. van Veenendaal and G.A. Sawatzky, Phys. Rev. Lett. **70**, 2459 (1993).
²⁰S.D. Peacor and T. Hibma, Surf. Sci. **301**, 11 (1994).
²¹C.T. Chen, F. Sette, Y. Ma, and S. Modesti, Phys. Rev. B **42**, 7262 (1990).
²²D. Alders, J. Vogel, C. Levelut, S.D. Peacor, T. Hibma, M. Sacchi, L.H. Tjeng, C.T. Chen, G. van der Laan, B.T. Thole, and G.A. Sawatzky, Europhys. Lett. **32**, 259 (1995).
²³F.M.F. de Groot, J.C. Fuggle, B.T. Thole, and G.A. Sawatzky, Phys. Rev. B **42**, 5459 (1990).
²⁴M. Tomellini, J. Chem. Soc. Faraday Trans. I **84**, 3501 (1988).
²⁵P. Kuiper, B.G. Searle, P. Rudolf, L.H. Tjeng, and C.T. Chen, Phys. Rev. Lett. **62**, 221 (1989).